Available online at www.sciencedirect.com

SciVerse ScienceDirect

Ceramics International 38 (2012) 1227–1233

CERAMICS INTERNATIONAL

www.elsevier.com/locate/ceramint

Synthesis and phase stability of precursor derived HfO_2/Si–C–N–O nanocomposites

Ravindran Sujith, Adhimoolam Bakthavachalam Kousaalya, Ravi Kumar *

Materials Processing Section, Department of Metallurgical and Materials Engineering, Indian Institute of Technology Madras, Chennai 600 036, India

Received 26 April 2011; received in revised form 8 August 2011; accepted 24 August 2011

Abstract

Hafnium alkoxide modified polysilazane was synthesized by the drop-wise addition of hafnium tetra(*n*-butoxide) to polysilazane. The solid state thermolysis (SST) temperature and the ceramic yield for both the polysilazane and modified polysilazane were determined by performing thermogravimetry. Fourier transform infrared spectroscopy was performed to understand the polymer to ceramic conversion as well as the bonding characteristics of the ceramics. The modified polymer after crosslinking was subjected to SST at 800 °C at a constant heating rate of 5 °C/min for a dwell time of 2 h in atmospheric ambience. From the X-ray diffractograms, the as-thermolysed ceramics were observed to remain X-ray amorphous and on heat-treatment resulted in the crystallization of tetragonal hafnia. However, on heat-treatment at 1500 °C, reverse phase transformation from tetragonal to monoclinic hafnia was observed. Raman spectroscopy and transmission electron microscopy were employed to further understand the phase evolution. The thermal stability and the influence of amorphous matrix on the coarsening of HfO_2 were also evaluated.

Keywords: A. Precursors: organic; B. Grain size; B. Microstructure-final; Diffusion

1. Introduction

Polymer precursor route for the synthesis of advanced ceramics has attracted considerable interest in recent years due to their exceptional high temperature stability, resistance to crystallization and thermal decomposition. Since these ceramics are essentially additive-free materials, they are found to exhibit extraordinary thermo-mechanical properties at elevated temperatures due to the absence of any low melting point phases [1–6]. In the last few years, significant research has gone into the development of Si-containing ternary systems such as silicon oxycarbide (Si–O–C) and silicon carbonitride (Si–C–N) ceramics with improved properties via polymer precursor route. In addition to the ternary systems, the development of quaternary and quinary silicon-based systems through polymer precursor route has also gained immense interest in the recent years. This involves incorporation of additional elements such as B [7–11], Al [12,13], Ti [14], Ta [15] or Zr [16–18] to the silicon-based polymer precursor thereby resulting in enhancement of properties and tunable performance.

The modification of the Si–C–O or Si–C–N by the incorporation of zirconium in the form of its oxide (ZrO_2) was observed to remarkably influence the properties of the polymer derived ceramics [16–18]. Recently, the incorporation of HfO_2 instead of ZrO_2 into the ceramic matrix is explored in the development of metal-oxide modified polymer derived ceramic [19–22]. Though ZrO_2 and HfO_2 are structurally very similar, HfO_2 is considered to be technologically more important because of its high melting point (2758 °C), high dielectric resistance [23,24], high neutron absorption capability [25] as well as its high chemical stability [26]. Both, HfO_2 and ZrO_2 undergo a series of phase transformation from monoclinic (space group: $P2_1/c$) to tetragonal (space group: $P4_2/nmc$) and from tetragonal to high symmetry cubic phase (space group: Fm3m). However, the transition temperatures were observed to be higher for HfO_2. The phase transformation temperature from monoclinic to tetragonal is close to 1670 °C for HfO_2whereas it is around 1170 °C for ZrO_2 and from tetragonal to cubic is 2670 °C and 2370 °C respectively [26]. This indicates the enhanced thermal stability of the HfO_2 modified system.

---

* Corresponding author. Tel.: +91 44 22574777; fax: +91 44 22574777.
E-mail address: nvrk@iitm.ac.in (R. Kumar).

0272-8842/$36.00
doi:10.1016/j.ceramint.2011.08.053

The influence of polymer architecture on the structural evolution of hafnium alkoxide modified polysilazane by comparing two variants of commercially available polysilazane was reported recently [22]. However, the influence of atmosphere and the effect of Si–C–N–O matrix on the structural evolution is not addressed. In this paper, we report the crystallization and microstructural evolution of HfO_2 from an amorphous matrix of Si–Hf–C–N–O and the influence of amorphous matrix and atmosphere on the thermal stability of the system. The thermal stability is determined by performing heat-treatment in air and inert atmosphere and the influence of surrounding matrix on microstructural evolution is determined by evaluating the crystallite sizes. The preliminary results indicate a promising potential of HfO_2 incorporated silicon-oxycarbonitrides (HfO_2/Si–C–N–O) with respect to carbothermal decomposition at elevated temperatures.

2. Experimental

2.1. Synthesis of polymer precursor

Hafnium alkoxide modified polymer precursor was synthesized by the chemical modification of polysilazane by the addition of hafnium tetra (*n*-butoxide) [$Hf(O^nBu)_4$] (Sigma Aldrich, India). To synthesize polysilazane, dichloromethylvinylsilane (Alfa Aesar, USA) was dissolved in tetrahydrofuran and taken in a three-necked round bottom flask maintained at 0 °C and connected to Schlenk line to maintain an inert atmosphere. The solution was ammonolysed by drop-wise addition of ammonia under vigorous stirring. After allowing the solution to reach room temperature, precipitated ammonium chloride was filtered and removed using Whatman glass microfiber filter paper to finally obtain a colorless and oily liquid [27]. The synthesized polysilazane was dissolved in toluene, and to which 30 vol% hafnium tetra (*n*-butoxide), dissolved in toluene, was added drop-wise at room temperature. Henceforth, the modified solution was subjected to continuous vigorous stirring for 24 h in argon atmosphere. Subsequently, the modified polymer was kept in the vacuum oven at 80 °C for 24 h, for the solvent to be removed. Finally, the modified polymer precursor was crosslinked at 200 °C in a programmable alumina tube furnace, maintaining a heating rate of 2 °C/min for 2 h in air.

2.2. Polymer to ceramic conversion

The crosslinked hafnium alkoxide modified polysilazane was thermolysed at 800 °C for 2 h in air. The SST was carried out in an alumina crucible placed in a programmable alumina tube furnace, maintained at a constant heating rate of 5 °C/min. Furthermore, the as-thermolysed ceramics were heat-treated in air at 1000, 1200, 1400 and 1500 °C maintaining the same heating rate as well as the dwell time for understanding the phase evolution. In order to determine the influence of atmosphere on the thermal stability of the system, the as-thermolysed ceramics were heat-treated in argon atmosphere at three different temperatures, namely, 1000, 1200 and 1400 °C for 2 h maintaining a heating rate of 5 °C/min till 1200 °C and 2°C/min beyond.

2.3. Characterization

Thermogravimetry (TG) analysis of the polysilazane and hafnium alkoxide modified polysilazane, was performed using NETZSCH STA 409 (Germany) under atmospheric ambience up to 1400 °C. Before performing TG, both the polymers were crosslinked at 200 °C in air. FT-IR of the hafnium alkoxide modified polysilazane as well as the unmodified polysilazane was recorded on a Perkin Elmer Spectrum one: FT-IR spectrometer, operated in the transmission mode. Furthermore, FT-IR was also performed on the as-thermolysed and heat-treated hafnia modified ceramics. The samples for FT-IR were prepared by pulverizing followed by thorough mixing with IR irradiated potassium bromide (KBr). The mixed powder was then pressed into a pellet, before it was observed in the spectrometer. The spectrum was taken in the scan range between 450 and 4500 cm^{-1} at a resolution of 4 cm^{-1}. All the spectroscopic measurements were performed at room temperature.

Powder XRD of the heat-treated samples were taken using D8 Discover, Bruker AXS X-ray diffractometer (USA), with Cu K_α radiation ($\lambda = 0.15408$ nm) in the 2θ range, 20–80°, at a scan rate of 1 s/step. The peaks were indexed with reference to powder diffraction files from the International Centre for Diffraction Data (ICDD) database. The full width half maximum (FWHM) for all the peaks was determined by fitting the peaks with standard pseudo-voigt function. Raman spectra of the powdered ceramic were taken using Labram HR 800, Horiba, (USA) Raman spectrometer with a laser source of He–Ne (632.8 nm) under 100× magnification. The samples were finely powdered and the spectrum was recorded in the range between 450 and 4000 cm^{-1}. For transmission electron microscopy (TEM) the powdered samples were dispersed in acetone by ultrasonicating for 10 min and a drop of the dispersed solution was deposited on a 3 mm carbon-coated copper grid using a dropper. TEM and high resolution-TEM (HR-TEM) images were taken using Philips-TEM (CM20) and JEOL 3010 (USA) respectively, both operated at an accelerating voltage of 200 kV by using finely powdered samples.

3. Results and discussion

Thermogravimetry of the polysilazane as well as the hafnium tetra(*n*-butoxide) modified polysilazane is shown in Fig. 1. The first derivative of TG (DTG) of hafnium alkoxide modified polysilazane, is also provided in the same figure (Fig. 1). The residual mass of the crosslinked polysilazane at 1400 °C, as understood from the TG is approximately 89%. However, for the hafnium alkoxide modified polysilazane crosslinked at 200 °C, the ceramic residue at 1400 °C is observed to be 80% approximately. The lower residue for the modified polysilazane can be attributed to the decomposition of hafnium tetra(*n*-butoxide) [19]. The DTG of the modified polysilazane exemplifies a three stage decomposition process

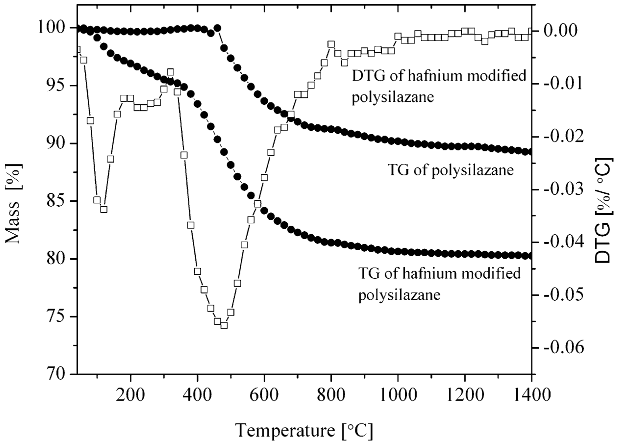

Fig. 1. Thermogravimetric (TG) analysis of non-modified polysilazane and the hafnium alkoxide modified polysilazane, both after crosslinking at 200 °C in air.

for the modified polysilazane, with peaks at 120, 220 and 480 °C approximately. The maximum mass loss (13% approximately) is observed during the third stage which can be attributed to the polymer to ceramic conversion. Beyond 800 °C, no significant mass loss is observed indicating the completion of ceramization.

The reaction mechanisms involved in the polymer to ceramic conversion are further understood by performing FT-IR analysis of the hafnium alkoxide modified polysilazane. Fig. 2 shows the FT-IR spectra of the unmodified polysilazane, as well as the hafnium alkoxide modified polysilazane. A broad and intense peak is observed in the spectrum of unmodified polysilazane (Fig. 2(a)) between 1200 and 1000 cm^{-1}, which is assigned to Si–O–Si bond, indicating inclusion of oxygen into the polymer chain due to possible oxygen contamination. Other bands related to Si–CH_3 and Si–C are observed at 1275 cm^{-1} and 790 cm^{-1} respectively. Besides, intense bands are observed at 3055 cm^{-1} (=CH_2), 2962 cm^{-1} (–CH_3), 1597 cm^{-1} (CH=CH_2), 1416 cm^{-1} (Si–CH_3 deformation) and 1260 cm^{-1} (Si–CH_3 stretching) [28]. A broad band is also observed between 3300 cm^{-1} and 3500 cm^{-1}, indicating the presence of N–H bonds. However, in the case of the unmodified polysilazane crosslinked at 300 °C (Fig. 2(b)) as well as in hafnium alkoxide modified polysilazane crosslinked at 200 °C (Fig. 2(c)), reduction in the intensity bands corresponding to vinyl bonds are observed signifying the occurrence of crosslinking. Also, a substantial reduction in the intensities of all–H containing peaks is observed for the sample processed at 600 °C (Fig. 2(d)), confirming the progress in the transformation of polymeric network to an amorphous pre-ceramic network.

Fig. 3 shows the FT-IR of the as-thermolysed as well as the heat-treated ceramic samples processed till 1500 °C. The presence of Si–O–Si bond (1200–1000 cm^{-1}) for the pyrolysed and heat-treated samples can be attributed to the processing atmosphere [29]. A less intense peak is observed for the thermolysed sample at 1600 cm^{-1}can be attributed to atmospheric or moisture contamination (R–OH) due to operation in air [30]. However, for the samples heat-treated at 1200 and 1500 °C, an evolution of new band in the FT-IR spectra at

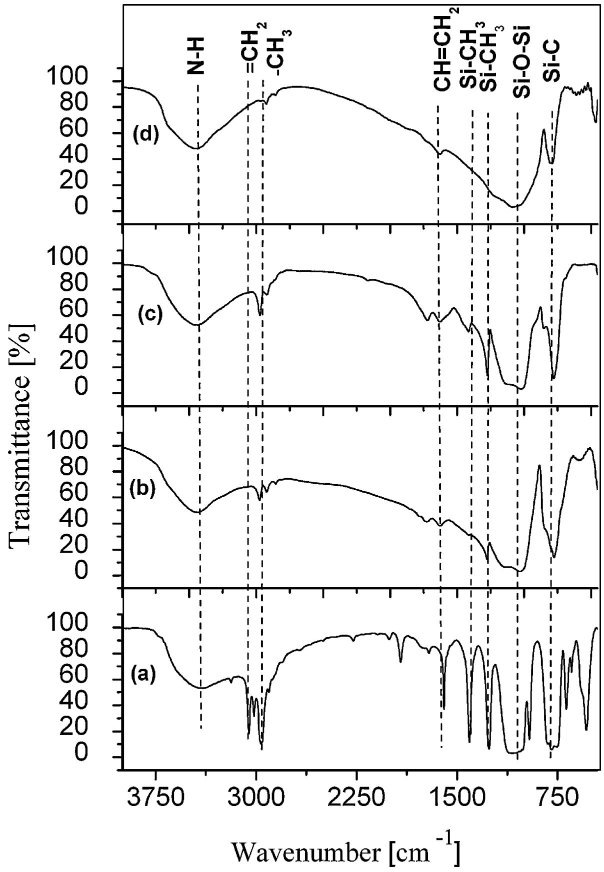

Fig. 2. Fourier-transformed infra red (FT-IR) spectra: (a) non-modified polysilazane, (b) non-modified polysilazane crosslinked at 300 °C, (c) hafnium alkoxide modified polysilazane crosslinked at 200 °C and (d) hafnium alkoxide modified polysilazane processed at 600 °C.

620 cm^{-1} can be observed. Also, reports suggest that regions between 250 and 1000 cm^{-1} in the FT-IR spectrum correspond to the stretching mode of Hf–O [31,32]. Hence, the corresponding band is assigned to Hf–O, indicating the phase separation of hafnia from the amorphous ceramic matrix.

Further understanding on the structural evolution of various phases from the ceramic matrix is obtained by performing XRD (Fig. 4). The powder XRD of the as-thermolysed ceramic indicates that the ceramic is completely X-ray amorphous. As inferred from the XRD, with increase in heat-treatment temperature, a progressive crystallization of nanocrystalline tetragonal hafnia is observed for the modified ceramics heat-treated up to 1400 °C. Though, thermodynamically monoclinic hafnia is the room temperature stable phase and tetragonal phase is stable only beyond 1670 °C [33], the presence of tetragonal hafnia can be attributed to the crystallite size effect [34,35]. The volume averaged crystallite size for tetragonal hafnia, as determined using Scherrer's formula is found to vary between approx. 3–10 nm (Fig. 5). An analysis using Williamson–Hall method [36] for the XRD of the heat-treated samples also indicates insignificant influence of microstrain on the crystallite broadening.

However, in the case of the as-thermolysed ceramic heat-treated at 1500 °C, as observed in XRD, the presence of monoclinic hafnia in addition to tetragonal hafnia can be

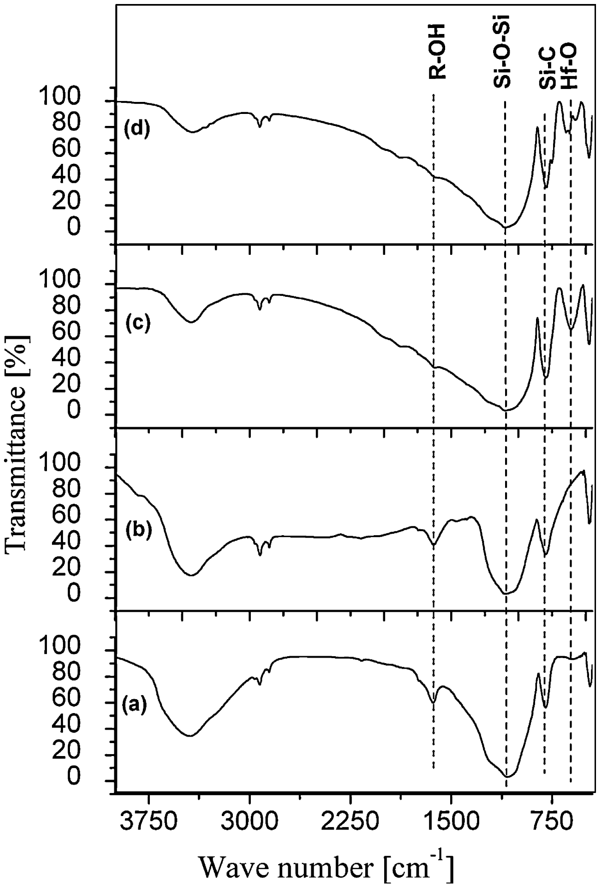

Fig. 3. Fourier-transformed infra red (FT-IR) spectra: (a) as-thermolysed Si–Hf–C–N–O, (b) Si–C–N–O ceramic heat-treated at 1200 °C, (c) HfO_2/Si–C–N–O ceramic heat-treated at 1200 °C and (d) HfO_2/Si–C–N–O ceramic heat-treated at 1500 °C.

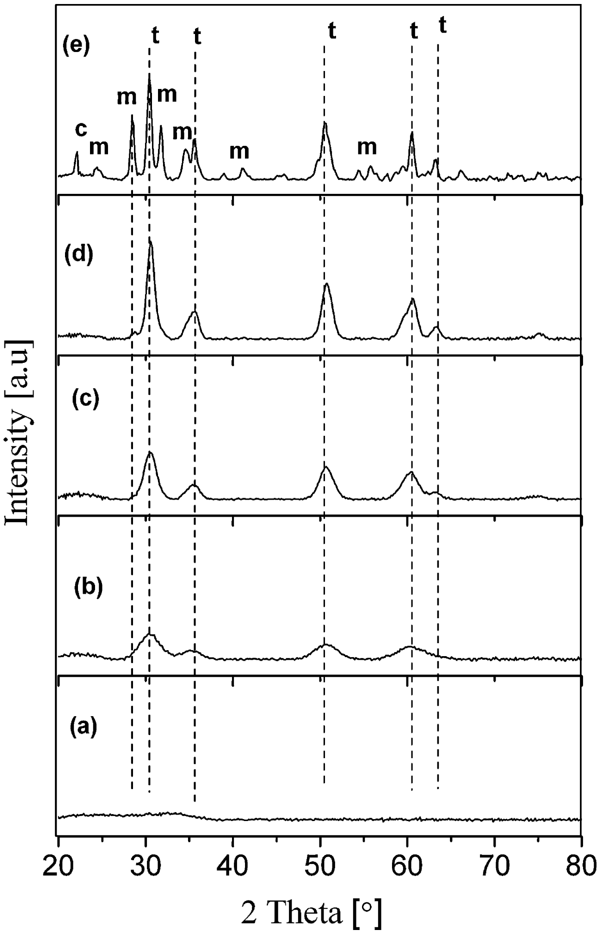

Fig. 4. Powder X-ray diffractogram (XRD) of HfO_2/Si–C–N–O ceramics: (a) as-thermolysed at 800 °C, (b) heat-treated at 1000 °C, (c) heat-treated at 1200 °C, (d) heat-treated at 1400 °C and (e) heat-treated at 1500 °C (c, crystobalite; t, tetragonal hafnia; m, monoclinic hafnia).

observed. This indicates that beyond a critical crystallite radius, tetragonal HfO_2 is unstable and gets transformed to monoclinic HfO_2. The critical crystallite radius necessary for the reverse phase transformation for hafnia to occur in an amorphous matrix of Si–C–N–O is observed to be 4 nm [37]. In this case, the volume averaged crystallite diameter for tetragonal hafnia (∼24 nm) as determined by Scherrer formula is found to be higher than critical radius of the crystallite and hence the phase transformation from tetragonal to monoclinic crystal structure.

Furthermore, the mass loss in % for the heat-treated hafnium alkoxide modified ceramic as well as the unmodified ceramics at various temperatures between 1000 and 1500 °C in air is determined and shown in Table 1. For Si–C–N–O ceramics, a mass gain of approximately 16% is observed on heat-treating at 1200 °C in air indicating excessive oxidation and formation of silica (SiO_2). This can be inferred from the powder XRD (Fig. 6) for the heat-treated ceramics at 1200 °C in atmospheric ambience. However, no significant mass loss is observed in the Si–Hf–C–N–O ceramic, upon heat-treating from 800 to 1000 °C for 2 h in air. Whereas, a progressive mass loss of approximately 15% is observed for the HfO_2/Si–C–N–O ceramic, upon heat-treating from 800 to 1500 °C for the same duration in air. This mass loss observed in the modified ceramic can be attributed to the presence of the free carbon in the ceramic matrix in addition to the heat-treatment atmosphere.

The presence of free carbon can be established from the Raman spectrum. Fig. 7 shows the Raman spectrum of the

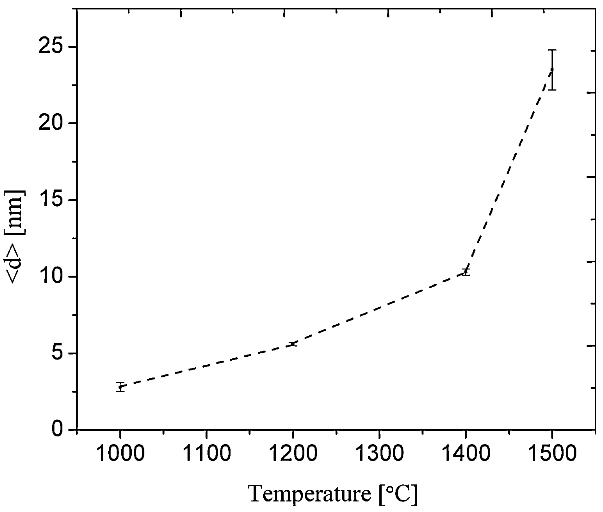

Fig. 5. Crystallite coarsening with variation in temperature. Dotted line is a guideline for eye.

Table 1
Variation in mass (%) upon heat-treatment temperature at various temperatures between 1000 and 1500 °C in air and argon.

Temperature (°C)	1000	1200	1400	1500
Si–C–N–O in air	*	∼+16	∼−6	*
Si–Hf–C–N–O in air	∼0	∼−5	∼−11	∼−15
Si–C–N–O in Ar	∼0	∼0	*	*
Si–Hf–C–N–O in Ar	∼0	∼0	∼−7	*

+ indicates mass gain, − indicates mass loss, * indicates not done.

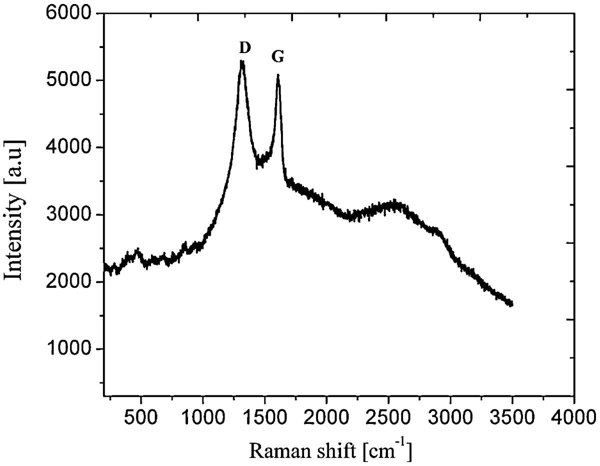

Fig. 7. Raman spectrum of HfO_2/Si–C–N–O thermolysed at 800 °C and subsequently heat-treated at 1200 °C for a dwell time of 5 h at a heating rate of 5 °C/min. Presence of D & G bands shows the presence of free carbon.

hafnium alkoxide modified ceramic heat-treated at 1200 °C for 5 h in air. The typical D & G absorption bands observed at 1360 cm^{-1} and 1600 cm^{-1}, indicate the presence of free carbon. Under ambient conditions, this free carbon will get easily oxidized and get evolved in the form of CO or CO_2, resulting in mass loss. In addition, the mass loss can also happen due to carbon coming into direct contact with SiO_2, leading to the dissociation of SiO_2 into SiO (g) and CO (g). Also, there could be a possible formation of SiC due to the reaction between silica and carbon which can also contribute to the mass loss. However, on heat-treating in Ar atmosphere both Si–C–N–O and the HfO_2/Si–C–N–O are observed to remain thermally stable up to 1200 °C (Table 1). The mass loss observed during the heat-treatment is found to be negligible indicating the influence of atmosphere on the decomposition behavior. This can be further inferred from the XRD (Fig. 6(c) and (d)) indicating the amorphous nature of the ceramic at these temperatures.

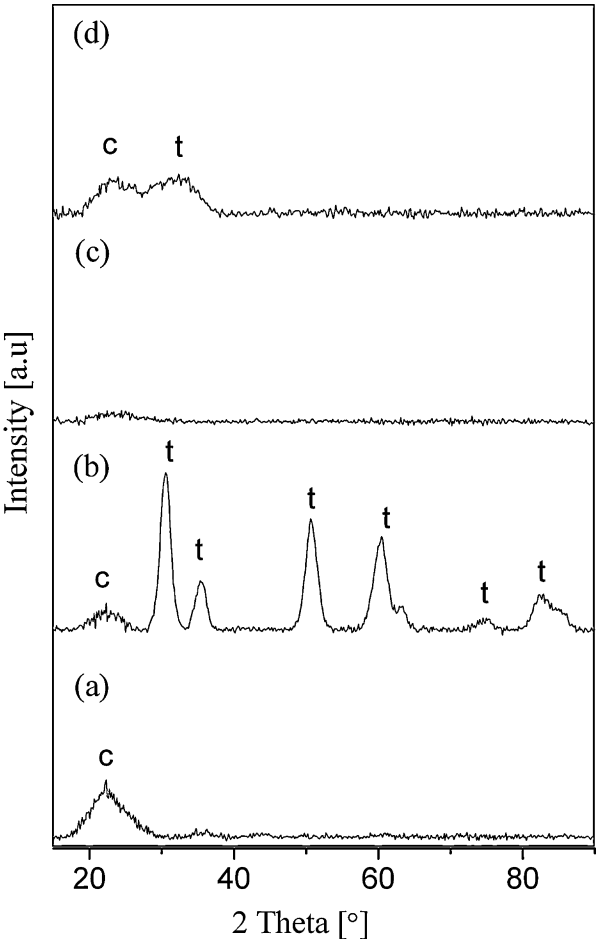

Fig. 6. Powder X-ray diffractogram (XRD) of HfO_2/Si–C–N–O and Si–C–N–O heat-treated at 1200 °C: (a) Si–C–N–O in air, (b) HfO_2/Si–C–N–O in air, (c) Si–C–N–O in Ar, (d) HfO_2/Si–C–N–O in Ar (c, crystobalite; t, tetragonal hafnia).

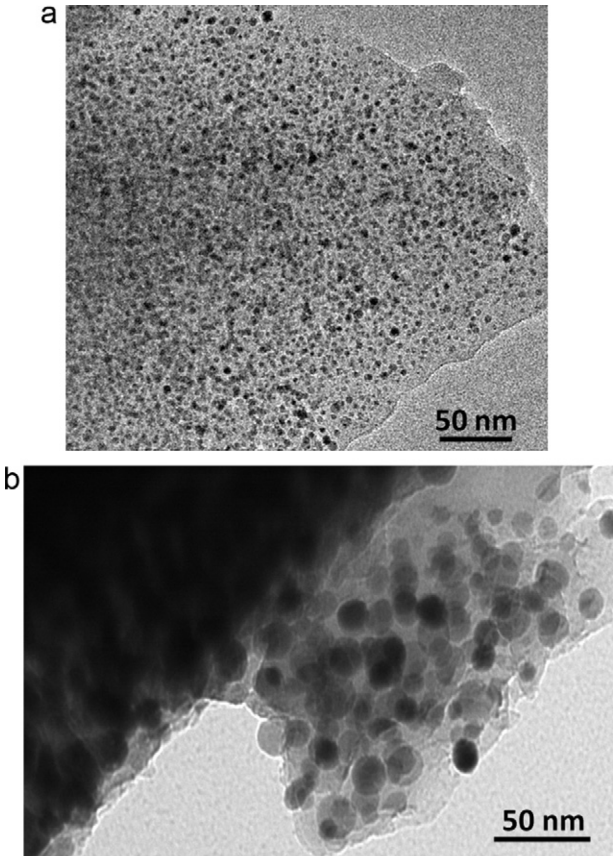

Fig. 8. (a) Transmission electron microscopy (TEM) image of HfO_2/Si–C–N–O thermolysed at 800 °C and subsequently heat-treated at 1200 °C for a dwell time of 5 h at a heating rate of 5 °C/min. (b) Transmission electron microscopy (TEM) image of HfO_2/Si–C–N–O thermolysed at 800 °C and subsequently heat-treated at 1400 °C for a dwell time of 10 h at a heating rate of 5 °C/min.

The presence of hafnia crystallites and the coarsening with heat-treatment can be further realized from the TEM images. The TEM image of the as-thermolysed ceramic heat-treated at 1200 °C (Fig. 8(a)) exemplifies the presence of crystallites of hafnia. The crystallite size as observed from the TEM image is found to vary between 5 and 8 nm which is very much in accordance with the crystallite size as determined using Scherrer's formula (Fig. 5). Fig. 5 indicates that there exists substantial resistance to crystallite coarsening during the early stages of nucleation and growth. However, at 1500 °C substantial coarsening of tetragonal hafnia is observed with a volume averaged crystallite size of $\sim$22 nm (Fig. 5). This could be also inferred from the TEM image for the modified ceramic heat-treated at 1400 °C for 10 h (Fig. 8(b)). This suggests that though coarsening is inevitable at higher temperatures, the presence of the amorphous matrix surrounding the crystallites can effectively increase the resistance to coarsening.

4. Conclusion

Si–Hf–C–N–O polymer derived ceramics were prepared by the thermolysis of hafnium alkoxide modified polysilazane. Upon thermolysis, the ceramics were found to remain X-ray amorphous and on further heat-treatment have resulted in the phase separation and crystallization of nanocrystalline tetragonal hafnia dispersed in an amorphous Si–C–N–O. From XRD and TEM it could be further understood that prolonged heat-treatment has resulted in considerable coarsening at elevated temperatures which eventually has resulted in the reverse phase transformation from tetragonal to monoclinic hafnia. Though mass loss is observed for the modified ceramic heat-treated under ambient conditions, the HfO_2/Si–C–N–O heat-treated in Ar atmosphere is observed to remain thermally stable up to 1200 °C.

Acknowledgements

We gratefully acknowledge Composites Technology Centre (COMPTECH), DST Unit of Nanoscience (DSTUNS) SAIF-IITM and Sophisticated Analytical Instruments Facility (SAIF), Indian Institute of Technology Madras for performing TG, HR-TEM and FT-IR respectively.

References

[1] S. Yajima, J. Hayashi, M. Omori, K. Okamura, Development of a silicon carbide fiber with high tensile strength, Nature 261 (1976) 683–685.

[2] Y. Wang, J. Ding, W. Feng, L. An, Effect of pyrolysis temperature on the piezoresistivity of polymer-derived ceramics, J. Am. Ceram. Soc. 94 (2) (2011) 359–362.

[3] L. Hu, R. Ceccato, R. Raj, Ultra figure-of-merit for hydrogen generation from sodium borohydride using ternary metal catalysts, J. Power Sources 196 (2011) 69–75.

[4] P. Colombo, G. Mera, R. Riedel, G.D. Soraru, Polymer derived ceramics: 40 years of research and innovation in advanced ceramics, J. Am. Ceram. Soc. 93 (7) (2010) 1805–1837.

[5] N.V. Ravi Kumar, S. Prinz, Y. Cai, A. Zimmermann, F. Aldinger, F. Berger, K. Muller, Crystallization and creep behavior of Si–B–C–N, Acta Mater. 53 (2005) 4567–4578.

[6] M. Gan, V. Tomar, Role of length scale and temperature in indentation induced creep behavior of polymer derived Si–C–O ceramics, Mater. Sci. Eng. A 527 (2010) 7615–7623.

[7] S.H. Lee, M. Weinmann, C_{fiber}/SiC_{filler}/Si–B–C–N $_{matrix}$ composites with extremely high thermal stability, Acta Mater. 57 (2009) 4374–4381.

[8] A.H. Tavakoli, P. Gerstel, J.A. Golczewski, J. Bill, Effect of boron on the crystallization of amorphous Si–(B)–C–N polymer derived ceramics, J. Non-Cryst. Solids 355 (2009) 2381–2389.

[9] Ravi Kumar, G. Rixecker, F. Aldinger, An elasticity of precursor derived Si–B–C–N ceramics, J. Eur. Ceram. Soc. 27 (2007) 1475–1480.

[10] Ravi Kumar, F. Phillip, F. Aldinger, Oxidation induced effects on the creep properties of nano-crystalline porous Si–B–C–N ceramics, Mater. Sci. Eng. A 445-446 (2007) 251–258.

[11] V. Petrman, J. Houska, S. Kos, P. Calta, J. Vlcek, Effect of nitrogen content on electronic structures and properties of SiBCN materials, Acta Mater. 59 (2011) 2341–2349.

[12] Y. Wang, Y. Fan, L. Zhang, W. Zhang, L. An, Polymer-derived Si–Al–C–N ceramics resist oxidation at 1400 °C, Scripta Mater. 55 (2006) 295–297.

[13] E. Bernardo, G. Parcianello, P. Colombo, J.H. Adair, A.T. Barnes, J.R. Hellmann, B.H. Jones, J. Kruise, J.J. Swab, SiAlON ceramics from preceramic polymers and nano-sized fillers: application in ceramic joining, J. Eur. Ceram. Soc. (2011), doi:10.1016/j.jeurceramsoc.2011.02.035.

[14] W. Acchar, F.C.C. Costa, M.R. Araujo, Ceramic composites derived from Ti/Al/Al_2O3-filled polysilsesquioxane, J. Adv. Res. Mech. Eng. 1 (2010) 70–72.

[15] E. Xie, S. Cao, J. Wang, X. Yan, S. Bernard, P. Miele, Engineering of silicon-based ceramic fibers: novel SiTaC(O) ceramic fibers prepared from polytantalosilane, Mater. Sci. Eng. A 527 (2010) 7086–7091.

[16] E. Ionescu, C. Linck, C. Fasel, M. Muller, H.J. Kleebe, R. Riedel, Polymer-derived SiOC/ZrO_2 ceramic nanocomposites with excellent high temperature stability, J. Am. Ceram. Soc. 93 (1) (2010) 241–250.

[17] A. Saha, S.R. Shah, R. Raj, Amorphous silicon carbide fibers drawn from alkoxide modified ceraset, J. Am. Ceram. Soc. 86 (8) (2003) 1443–1445.

[18] A. Saha, S.R. Shah, R. Raj, Oxidation behavior of SiCN–ZrO_2 fiber prepared from alkoxide modified polysilazane, J. Am. Ceram. Soc. 87 (8) (2004) 1556–1558.

[19] E. Ionescu, B. Papendorf, H.J. Kleebe, F. Poli, K. Muller, R. Riedel, Polymer-derived silicon oxycarbide/hafnia ceramic nanocomposites. Part I. Phase and microstructure evolution during the ceramization process, J. Am. Ceram. Soc. 93 (6) (2010) 1774–1782.

[20] E. Ionescu, B. Papendorf, H.J. Kleebe, R. Riedel, Polymer-derived silicon oxycarbide/hafnia ceramic nanocomposites. Part II. Stability toward decomposition and microstructure, J. Am. Ceram. Soc. 93 (6) (2010) 1783–1789.

[21] S. Brahmandam, R. Raj, Novel composites constituted from hafnia and a polymer derived ceramic as an interface: phase for severe ultrahigh temperature applications, J. Am. Ceram. Soc. 90 (10) (2010) 3171–3176.

[22] B. Papendorf, K. Nonnenmacher, E. Ionescu, H.J. Kleebe, R. Riedel, Strong influence of polymer architecture on the microstructural evolution of hafnium alkoxide modified silazanes upon ceramization, Small 7 (7) (2011) 970–978.

[23] R.D. Robinson, J. Tang, M.L. Steigerwald, L.E. Brus, I.P. Herman, Raman scattering in $Hf_xZr_{1-x}O_2$ nanoparticles, Phys. Rev. B 71 (2005), 115408 (1–8).

[24] M. Shandalov, P.C. McIntyre, Size dependent polymorphism in HfO_2 nanotubes and nanoscale thin films, J. Appl. Phys. 106 (2009) 084322.

[25] D.R. Spink, J.H. Schemel, The development of rare earth pyrohafnates for power reactor control rod materials, J. Nucl. Mater. 49 (1) (1973/74) 1–9.

[26] X. Zhao, D. Vanderbilt, First principle study of structural, vibrational and lattice dielectric properties of hafnium oxide, Phys. Rev. B 65 (2002) 233106.

[27] A. Müller, P. Gerstel, M. Weinmann, J. Bill, F. Aldinger, Si–B–C–N ceramic precursor derived from dichlorodivinylsilane and chlorotrivinylsilane. 1. Precursor synthesis, Chem. Mater. 14 (2002) 3398–3405.

[28] R. Li, C. Zhou, L. Yang, S. Li, J. Zhan, Z. Yu, H. Xia, Synthesis and polymer- to-ceramic conversion of tailorable polysilazanes, J. Appl. Polym. Sci. (2011), doi:10.1002/app.34274.

[29] R. Chavez, E. Ionescu, C. Balan, C. Fasel, R. Riedel, Effect of ambient atmosphere on crosslinking of polysilazanes, J. Appl. Polym. Sci. 119 (2011) 794–802.

[30] N. Janakiraman, F. Aldinger, Fabrication and characterization of fully dense Si–C–N ceramics from a poly(ureamethylvinyl)silazanes, J. Eur. Ceram. Soc. 29 (2009) 163–173.

[31] S.X. Lao, R.M. Martin, J.P. Chang, Plasma enhanced atomic layer deposition of HfO_2 and ZrO_2 high-k thin films, J. Vac. Sci. Technol. A 23 (3) (2005) 488–496.

[32] D.A. Neumayer, E. Cartier, Materials characterization of ZrO_2–SiO_2 and HfO_2–SiO_2 binary oxides deposited by chemical solution deposition, J. Appl. Phys. 90 (4) (2001) 1801–1808.

[33] D. Shin, R. Arroyave, Z.K. Liu, Thermodynamic modeling of the Hf–Si–O system, Calphad 30 (2006) 375–386.

[34] R.C. Garvie, The occurrence of metastable tetragonal zirconia as a crystallite size effect, J. Phys. Chem. 69 (1965) 1238–1243.

[35] O. Hunter Jr., R.W. Scheidecker, S. Tojo, Characterization of metastable tetragonal hafnia, Ceram. Int. 5 (4) (1979) 137–142.

[36] G.K. Williamson, W.H. Hall, X-ray line broadening from filed aluminium and wolfram, Acta Mater. 1 (1953) 22–31.

[37] R. Sujith, A.B. Kousaalya, Ravi Kumar, Coarsening induced phase transformation of hafnia in polymer derived Si–Hf–C–N–O ceramics, J. Am. Ceram. Soc., doi:10.1111/j.1551-2916.2011.04719.x, in press.